

HETEROSTRUCTURES BASED ON SMALL MOLECULES ORGANIC COMPOUNDS

M. SOCOL^{a*}, O. RASOGA^a, C. BREAZU^{a,b}, G. SOCOL^c, N. PREDA^a, I. PASUK^a, D. VISAN^b, I. STAVARACHE^a, F. GHERENDI^c, M. GIRTAN^d, U. SIDWABA^e

^aNational Institute of Material Physics, 105 bis Atomistilor Street, 077125, Bucharest-Magurele, Romania

^bUniversity of Bucharest, Faculty of Physics, 405 Atomistilor Street, 077125, Bucharest-Magurele, Romania

^cNational Institute for Lasers, Plasma and Radiation Physics, 409 Atomistilor Street, 077125, Bucharest-Magurele, Romania

^dLaboratoire de Photonique d'Angers, Université d'Angers, 2, Bd. Lavoisier, 49045, Angers, France

^eDepartment of Chemistry, University of the Western Cape, Bellville, 7535, Cape Town, South Africa

Heterostructures with layers from small molecules organic compounds were deposited on ITO/glass substrate by thermal vacuum evaporation (TVE) technique. Structural, optical and morphological investigations were carried out on the realised layers (zinc phthalocyanine-ZnPc, fullerene-C60 and 1,4,5,8-naphthalene-tetracarboxylic dianhydride-NTCDA). The films are polycrystalline keeping the morphological features characteristic to these materials. The prepared heterostructures reveal a large absorption domain in the visible domain. The current-voltage (I-V) characteristics of the investigated structures, recorded in dark, present an improvement in the current value (~ one order of magnitude) for the standard structure (ITO/PEDOT:PSS/ZnPc/C60/NTCDA/Al) with a supplementary layer of poly(3,4-ethylenedioxythiophene)-poly(styrenesulfonate) (PEDOT:PSS). For the inverted structure (Al/NTCDA/C60/ZnPc/ITO) was also noticed an increased current value in comparison with that observed for the standard structure.

(Received October 30, 2015; Accepted December 4, 2015)

Keywords: Small molecules compounds, TVE method, Metal phthalocyanine, Fullerene, Inverted structure

1. Introduction

In the last years organic materials were intensely studied due to the possibility to replace the inorganic materials in different applications, such as: organic photovoltaic cell-OPV, organic field effect transistor-OFET, organic light emitting devices-OLED [1-10]. The interest is owed to the decreased manufacturing cost (compared to the inorganics), this being associated with the variety of the methods available for their processing.

Over the time, due to its good transparency and low resistivity, ITO remains, the most used transparent conductor electrode (TCE) into the OPV and OLED architecture [11, 12]. Moreover, the OPV parameters (short-circuit current- I_{SC} , fill factor-FF) can be improved by adding to ITO, a buffer layer as poly(3,4-ethylenedioxythiophene)-poly(styrenesulfonate) (PEDOT:PSS) which is characterised by a higher work function. This material with "p" type conduction and with an ionisation potential nearest to ITO work function facilitates the injection of the holes in the organic material [12].

* Corresponding author: marcela.socol@infim.ro

Also, the researcher attention was oriented to the fabrications of OPV based on small molecules due to possibility to control very well the thickness of the films and due to the chemical stability of these materials such as zinc phthalocyanine (ZnPc) and magnesium phthalocyanine (MgPc) [12]. Metal phthalocyanines (MPc) are part from the small molecules class having Q-band absorption in the red to near-IR range and photovoltaic properties. They act as donor materials into an organic solar cell structure [13]. From these compounds, ZnPc is more utilized in OPV having the absorption coefficient around $1.5 \times 10^5 \text{ cm}^{-1}$ in the 600-750 nm wavelength range [14]. The ZnPc electronic affinity is $\sim 3.28 \text{ eV}$ and the ionisation potential is $\sim 5.28 \text{ eV}$ [15].

Fullerenes are highly symmetric cage molecules with many applications in: electronics, magnetics, superconducting, medicine, biochemistry [16]. From fullerenes, C60 molecule was found to be stable, with low interactions with other molecules. The C60 stability is partially due to the 7.4 eV binding energy per carbon atom [17]. Into an OPV configuration, C60 is used as electron acceptor layer having a relatively high electron mobility (up to $1 \text{ cm}^2/\text{Vs}$) [1], LUMO at 3.7 eV and HOMO at 6.2 eV [18].

Due to the favorable energy levels, a donor-acceptor junction can be formed using ZnPc and C60. Molecules with an aromatic π -system, C60 and phthalocyanines are promising building molecular materials with electrochemical and photo physical properties [19].

1,4,5,8-naphthalene-tetracarboxylic dianhydride-NTCDA is another small molecules organic material characterised by a highly symmetry, with planar and π -conjugated molecules [20]. Transparent as thin layer, with „n” conduction type, was used as buffer layer in the heterostructure with staked layers, before the deposition of the metallic cathode. It is a wide energy gap material ($E_g \sim 4 \text{ eV}$ determinate from the HOMO-8 eV and LUMO-4 eV position [18]) that can protect the investigated heterostructure from electrically shorting-out which can appear at the penetration of the hot metal atoms deposited by TVE. Also, NTCDA can act as an exciton blocking layer (EBL) avoiding the quenching of the excitons generated in the acceptor layer [18,21].

To complete the heterostructure a metal should be deposited on top. From the metals (Au, Ag, Al, Cu, etc) the most used was the Al due to its low work function ($W_{F_{Al}} = 4.7 \text{ eV}$ [22]). However, the Al can diffuse into the active layer acting as a recombination site [13]. In literature was reported that is better to use an inverted structure which is found to be more stable comparatively with the same structure in the standard configuration [23, 24].

In this context, the present work is focused on a comparative study regarding some organic heterostructures in the standard and in the inverted configurations based on ZnPc, C60 and NTCDA.

2. Experimental

ZnPc, C60 and NTCDA (Aldrich) active layers were deposited by thermal vacuum evaporation (TVE) method using an Alcatel system with turbo molecular pump. Details about this deposition technique are given in [15]. The deposition processes were made in the chamber at a starting pressure from $1.1 \times 10^{-5} \text{ mbar}$ until to $8 \times 10^{-6} \text{ mbar}$. The evaporation temperature (monitored with a thermocouple) during deposition was: $(210-218)^\circ\text{C}$ for ZnPc, $(245-255)^\circ\text{C}$ for C60 and $(156-166)^\circ\text{C}$ for NTCDA. ITO/glass, PEDOT:PSS/ITO/glass, silicon and glass were used as substrates in our experiments. Prior to the deposition, the glass/ITO cleaned substrates ($15 \Omega/\text{sq}$) were treated in oxygen plasma in order to improve the adherence of the materials.

Spin-coating (Chemat Technology instrument) technique was used to deposit the PEDOT:PSS layer (20 nm) on ITO at 3000 rot/min rotation speed for 30s. Further, the obtained layer was exposed to a thermal treatment at 120°C for 5 min to improve the quality of the film.

A SPECTROS system Spectros from Kurt J. Lesker have been used for the deposition by TVE of the aluminum (Al) electrodes with a 80 nm thickness ($4\text{\AA}/\text{s}$ deposition rate at 10^{-4} Pa pressure in the chamber). A quartz crystal monitor was involved in the thickness control.

The heterostructures were prepared in standard configuration with the glass/ITO electrode at the bottom and with the Al as top contact and in the inverted with the glass/Al at bottom and with the ITO deposited by pulsed laser deposition (PLD technique above. In the standard

configuration, two heterostructure types were investigated: ITO/PEDOT:PSS(20 nm)/ZnPc(52 nm)/C60(20 nm)/NTCDA(120 nm)/Al and ITO/ZnPc(50 nm)/C60(28 nm)/NTCDA(111 nm)/Al). In the inverted structure the ITO top contact was deposited by PLD method using an excimer laser source with KrF* (Coherent, CompexPro 205) operating at $\lambda=248$ nm, with $\tau_{FWHM} \sim 25$ ns. The deposition were made at room temperature at 5 Hz repetition rate. The number of the laser pulses was 30000. The deposition chamber was filled with oxygen at 1.5 Pa pressure. Details about the deposition method and system are given in the reference [25,26]. The ITO target (SCI Engineered Materials) was rotated during the deposition in order to prevent the local deterioration. In the same deposition cycle, besides the sample with the organic layers was inserted a simple glass substrate to be covered with ITO. This sample was used to measure the resistivity of the obtained ITO layer ($\rho=3.9 \text{ E-4 } \Omega\text{cm}$). The inverted structure obtained was: glass/Al/NTCDA(90)/C60(20)/ZnPc(52)/ITO.

From morphological point of view the heterostructures were analyzed by SEM (Hitachi S3400) and by AFM (Nanonics MultiView 4000 working in phase feedback). On a Bruker D8 Advances instrument were obtained the XRD diffractograms of the thin films deposited on glass. The set-up has monochromatized Cu $K_{\alpha 1}$ radiation ($\lambda=1.4506 \text{ \AA}$) and use a Bragg-Bretano geometry. The XRD diffractograms were recorded in 5° - 55° domain with a 0.04° step size and 2.5 s/step.

FTIR spectroscopy (Shimadzu 800 Spectrometer) was used to verify if changes in the sources material composition could appear during the organic material deposition. UV-VIS spectra (double beam CINTRA 10e GBC Spectrophotometer) were recorded in the 280 nm-800 nm domain. Electrical measurements were performed in dark using a Keithley 2611A SourceMeter Unit coupled at 2 microprobe Zuss PH-100.

3. Results and discussion

In the case of the thin films the morphology is a very important aspect, the charge carrier transport being affected by the roughness. The SEM and the AFM images of the single films (ZnPc, C60 and NTCDA) on glass substrate and of the stacked films in the standard (glass/ZnPc/C60/NTCDA) and in the inverted (glass/NTCDA/C60/ZnPc) configurations are observed in the Figure 1 and 2. The AFM roughness parameters are given in the Figure 2.

ZnPc layer has a similar topography to the other films reported for this material [27-29] and is characterized by a low RMS/Ra values (5.13 nm/4.08 nm) compared with those obtained for other materials investigated in this paper. The C60 film shows the specific morphology of the films prepared by TVE [30], having specific nanostructures [16, 31] with a higher roughness (14.67 nm/11.54 nm) although the thin film is thinner (20 nm) than the ZnPc film. This roughness may be attributed to the conformation of the C60 molecule. The highest roughness (20.92 nm/16.52 nm) was obtained for the NTCDA layer being linked to the layer thickness.

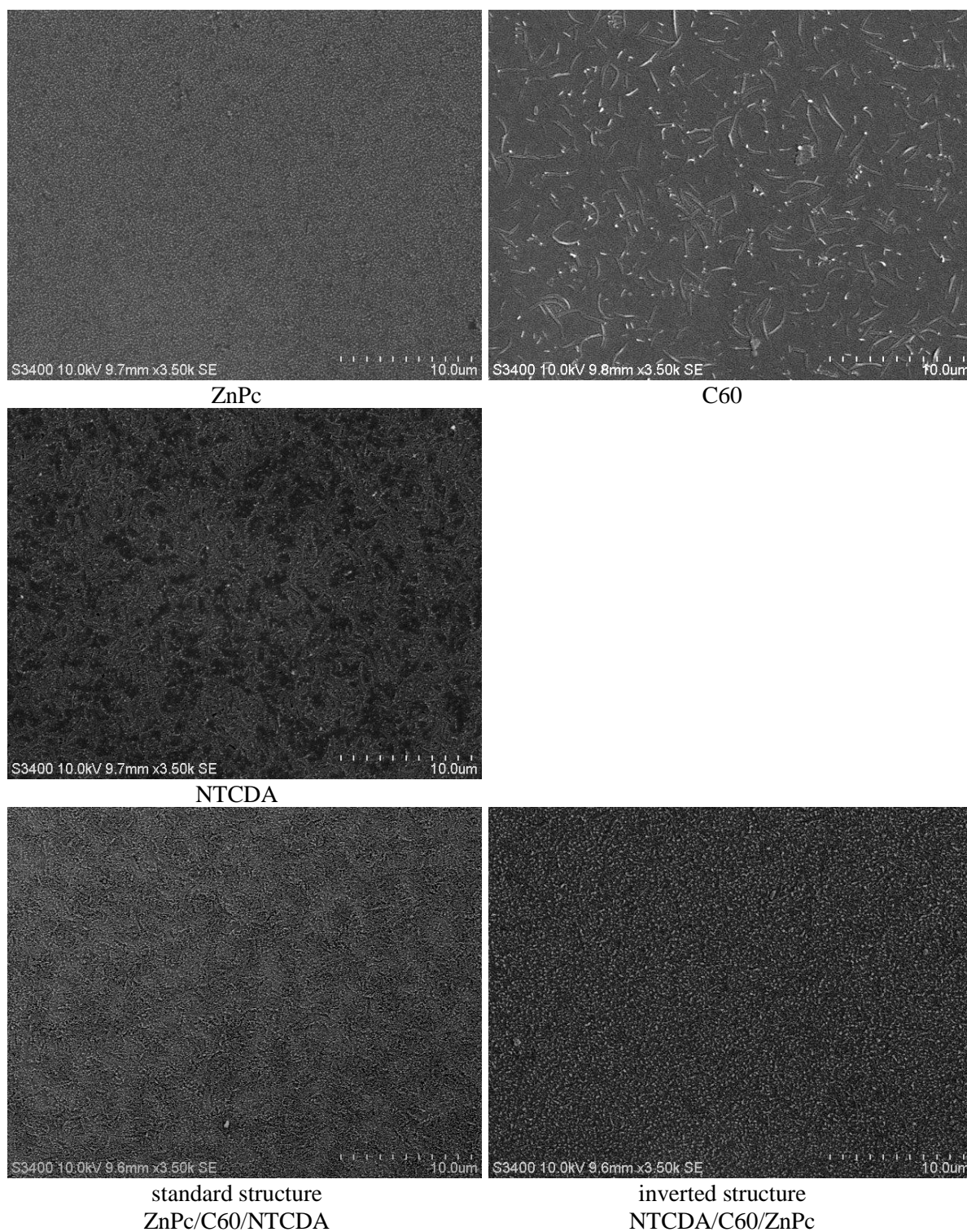


Fig. 1: SEM images of the single layers, the standard and the inverted structures

Scanning the surface of the materials in inverted structure it can be noticed that the final obtained roughness was smaller (6.75 nm/5.38 nm) compared to that of the single layers. Probably the high roughness obtained for the C60 layer favors a better accommodation of the NTCDA molecule than in the case when Al/glass was used as substrate.

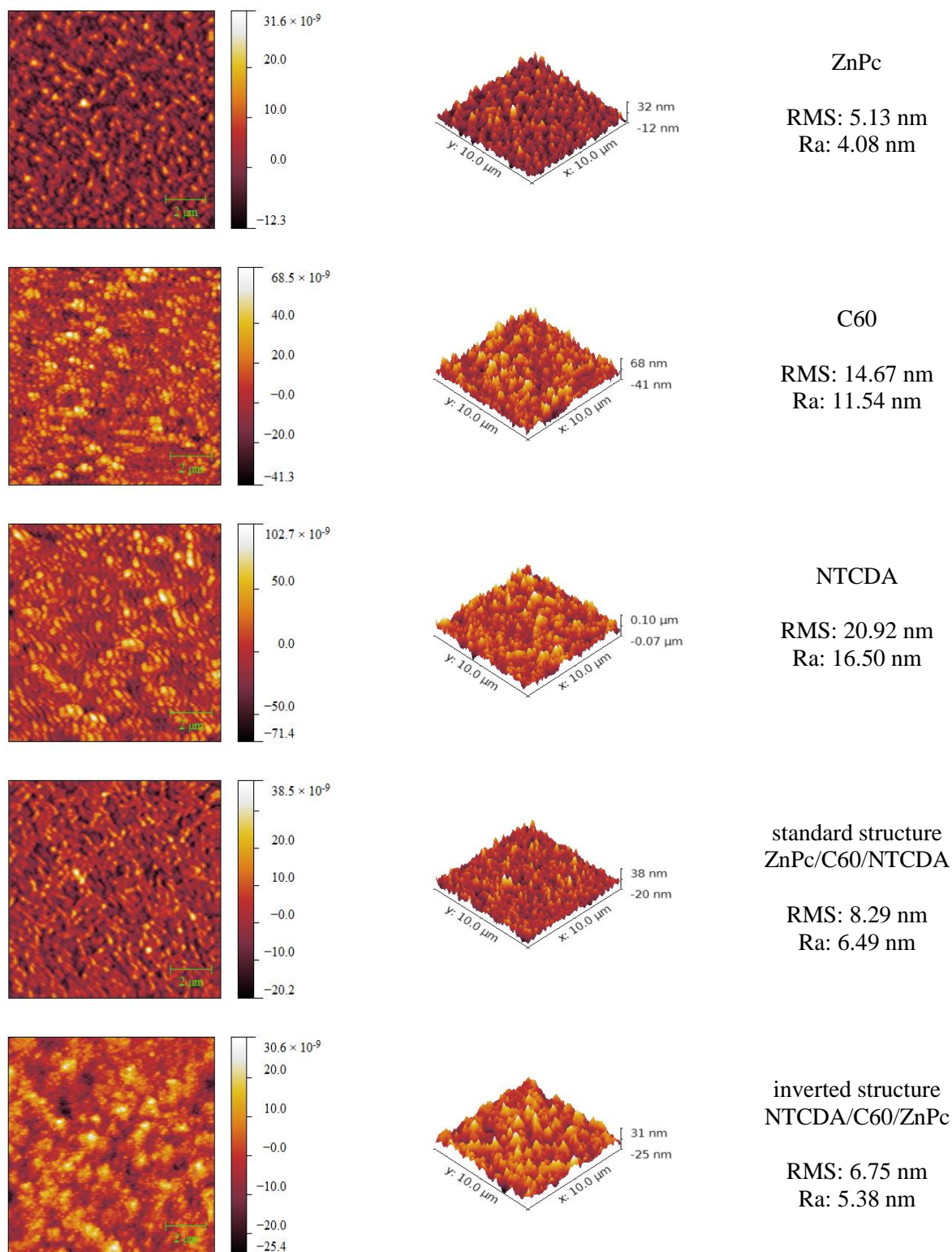


Fig. 2: AFM images of the single layers, the standard and the inverted structures

From the XRD diffractograms (Figure 3) it can be observed that the obtained films are not completely amorphous. In the case of the ZnPc films we found the signature of the initial material, although the intensity of the diffraction peaks situated at: 6.9° , 9.6° , 29.3° [29] is reduced (probably due to the film thickness). Also, the C60 film is polycrystalline presenting lines at 11.8°

and 23.7° corresponding to the (111) and (311) diffraction planes [32]. Due to the fact that, after our knowledges in literature are not reported data regarding the structure of the NTCDA, we show the XRD diagrams both for this compound as film and also as powder. Some of the obtained lines are observed in the both samples, more intense being that from 11.9° . As well, in the XRD diagrams of the investigated structures (Figure 3c) can be observed this characteristics line of NTCDA, more intense in the inverted structure where this layer is situated on the top of the structure.

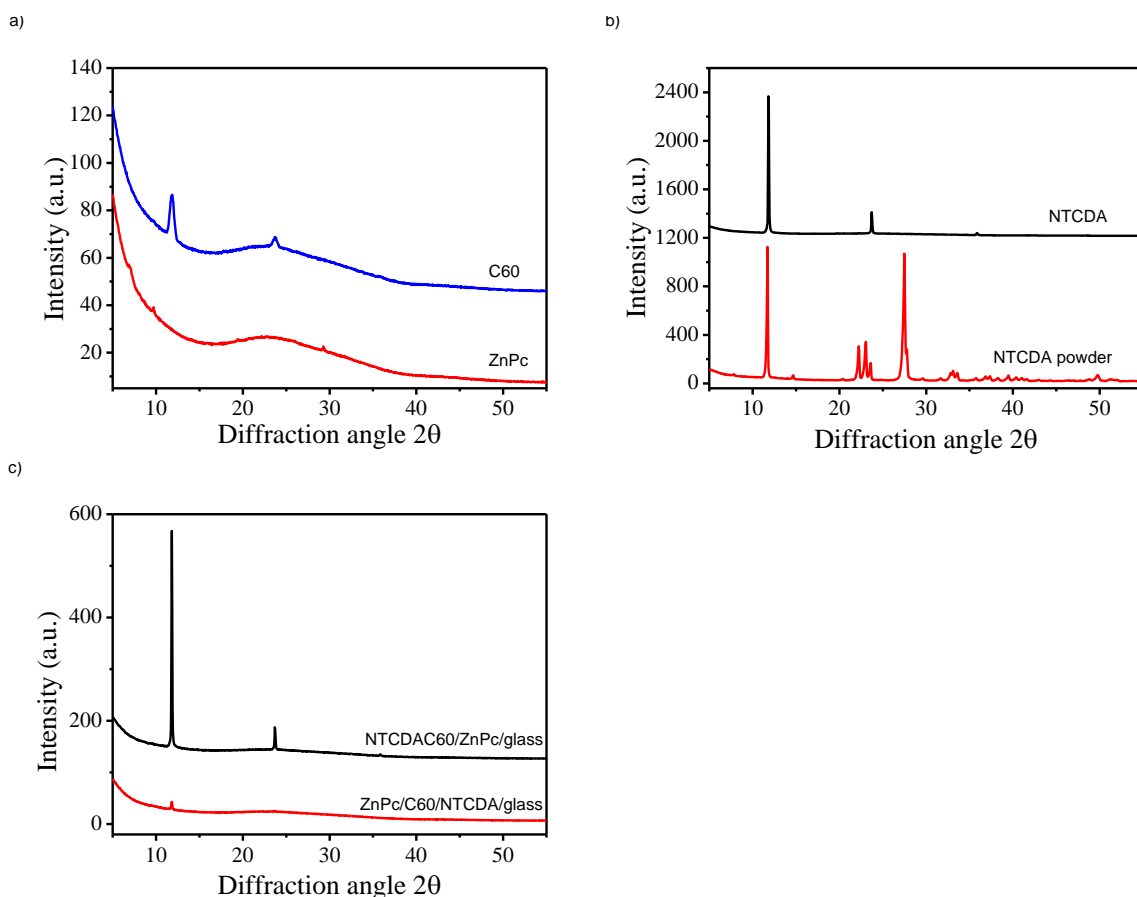


Fig. 3: XRD diffractograms of the ZnPc film, C60 film, NTCDA film and powder, and of the standard and inverted structures

The FTIR spectra of the ZnPc and NTCDA layers are presented in the Figure 4. For the metal phthalocyanines film the most important vibrations appear between 500 cm^{-1} and 1700 cm^{-1} . The intense peak from 727 cm^{-1} is attributed to out of plane deformation of C-H. Other peaks can be found at 748 cm^{-1} , 1095 cm^{-1} , 1118 cm^{-1} , 1288 cm^{-1} and are assigned to in-plane C-H bending. The C-C stretching in isoindole is indicated at 1333 cm^{-1} . The peaks from 1481 cm^{-1} and 1608 cm^{-1} are due to the C=C benzene stretch [28, 33]. The FTIR spectrum for the C60 layer is not presented taking into account the reduced thickness of the layers, the characteristic four bands of the C60 powder from 525 cm^{-1} , 575 cm^{-1} , 1181 cm^{-1} , 1428 cm^{-1} [34] were not identified in the film. The spectra of the TVE obtained NTCDA layer present the characteristic strong peak situated at 1780 cm^{-1} , assigned to the dianhydride carbonylic group [35]. The intense peaks from 543 cm^{-1} , 753 cm^{-1} and 882 cm^{-1} are attributed to the out-of-plane C-H bending vibrations [20, 36]. Also, the weaker peaks from 698 cm^{-1} and 754 cm^{-1} are assigned to the same C-H bending vibration [36]. The C-O stretching vibration of the anhydride groups and the in-plane C-H bending vibration introducing peaks at 1044 cm^{-1} , 1120 cm^{-1} , 1161 cm^{-1} , 1234 cm^{-1} and at 1293 cm^{-1} . The peaks characteristic to the C=C bending vibrations appear at 1442 cm^{-1} and at 1582 cm^{-1} [36]. Due to the fact that we saw in the FTIR spectra of the ZnPc and NTCDA the characteristics vibrations of the

source materials we conclude that no chemical decomposition take place during the thermal vacuum evaporation deposition.

In the Figure 5 is illustrated the UV-VIS spectra of the organic layers. The ZnPc layer show a higher transparency $\sim 90\%$ (at 500 nm), close to that of used glass substrate. The transparency of this film cover a large part of the VIS region, the transmittance spectrum presenting the characteristic B band (Soret) and Q band [27, 37]. As can be observed in the C60 spectra the thin film has several absorption bands situated in the short-wavelength range (~ 342 nm, ~ 400 nm, ~ 440 nm), bands characteristic to this material deposited by thermal evaporation [30, 38, 39].

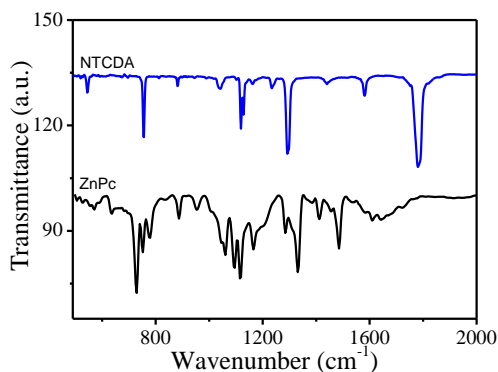


Fig. 4: FTIR spectra of the ZnPc and NTCDA single layers

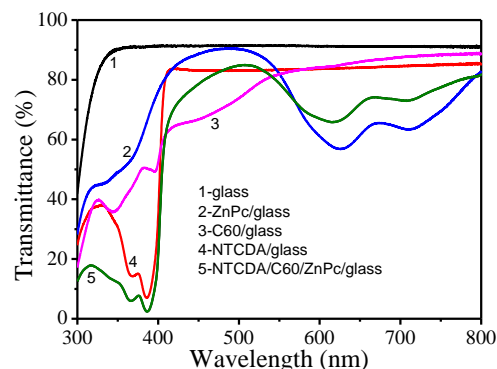


Fig. 5: UV-VIS spectra of the thin films and of the standard structure

As was expected (Figure 5-curve 4), the NTCDA film has absorption just in the UV part of the solar spectrum, this material being a wide gap organic [40]. Usually, the UV-VIS spectrum of this compound present absorption at 367 nm and 388 nm, absorption due to the symmetry-allowed π - π^* transition [41]. In the present case, the NTCDA was used just as a buffer layer between the acceptor layer (C60) and the cathode. In the UV-VIS spectrum of the structure formed by the superposition of the investigated three layers (NTCDA/C60/ZnPc) we saw that the transparency is still high at the 500 nm wavelength and cover a large part of the UV-VIS spectrum.

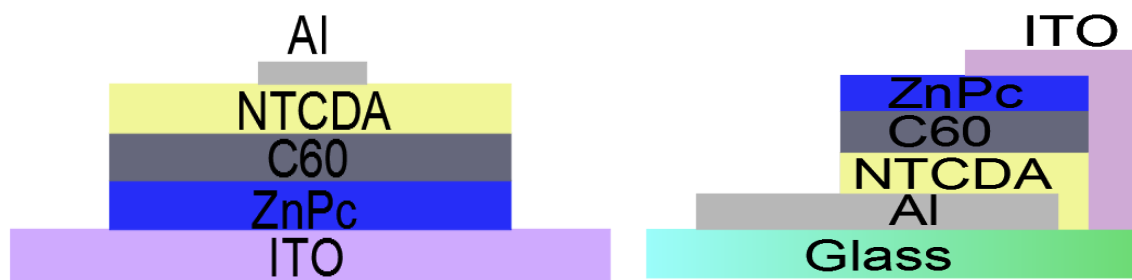


Fig. 6: Schematic representation of the standard and inverted structures

For a better understanding of the investigated heterostructures, schematic representations of the standard and of the inverted configurations are given in the Figure 6.

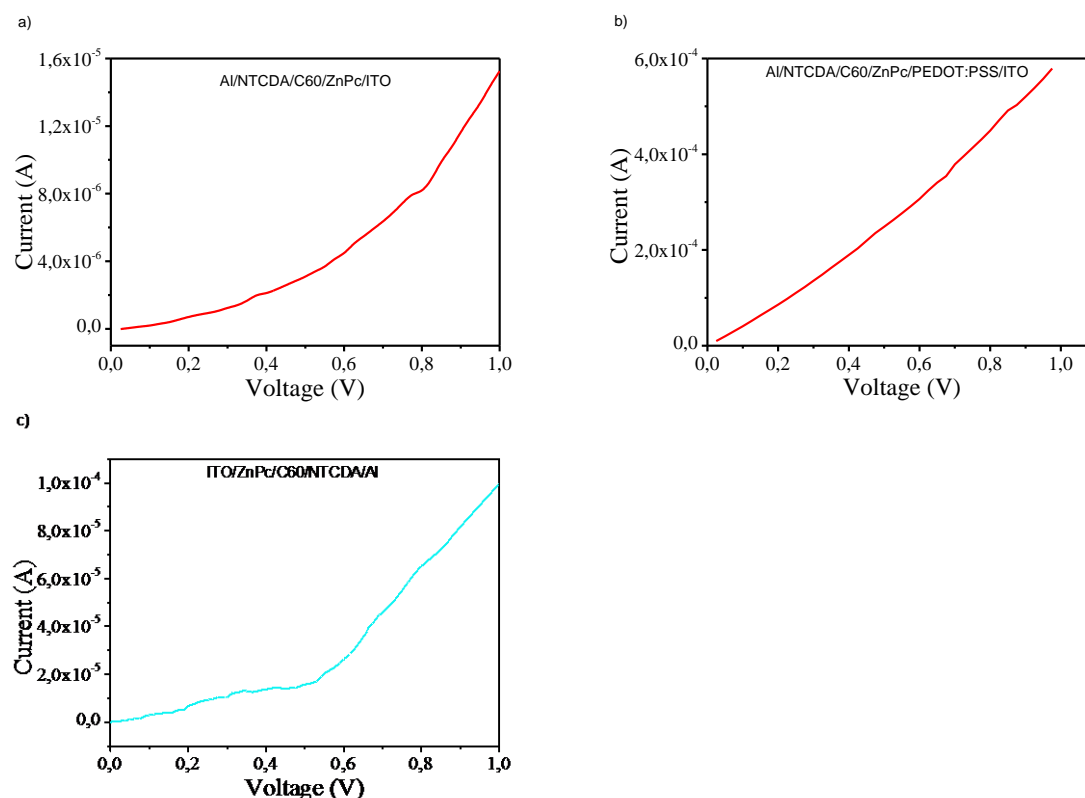


Fig. 7: I-V characteristics of the organic heterostructures: a) standard structure; b) standard structure with a suplimentary layer of PEDOT:PSS and c)inverted structure

The I-V characteristic (Figure 7) recorded in dark condition are plotted in (0-1) V range. The obtained values for the current are characteristic to the organic thin films. A suplimentary layer of PEDOT:PSS in the standard structure (ITO/PEDOT:PSS/ZnPc/C60/NTCDA/Al) lead to an increase in the current value in the structure, from 1.6×10^{-5} A at 6×10^{-4} A (at least with one order of magnitude). This behavior was expected due to the fact that is known that a thin layer from PEDOT:PSS facilitate the hole injection in the organic layer [12]. Using a inverted structure, an improvement in the current was also observed, from 1.6×10^{-5} A at 1×10^{-4} A (\sim one order of magnitude). This difference can appears due to the fact that is better to deposit an organic material on Al instead to deposit the Al on the top of the organic, taking into account the chemical interaction between the Al atoms and the organic layer which have as result the appearance of the recombination centers at the interface [42]. Also these two structures are different from morphological point of view, the standard structure being characterized by larger roughness parametres compared to the standard one (Figure2), this aspect being very important for the charge carrier transport into these type of structures.

4. Conclusions

Thin layers based on ZnPc, C60 and NTCDA were successfully deposited by TVE. The organic films are polycrystalline and are characterised by a low roughness (RMS/Ra ranged between: 5.1/4 nm and 20.9/16.5 nm). The films morphologies are characteristic to the investigated materials (ZnPc, C60 and NTCDA) and similar with those reported in the literature. The obtained films preserve the optical properties of the investigated materials, presenting high transparency in the visible part of the solar spectrum. The FTIR spectra show the characteristic vibrations of the ZnPc and NTCDA, confirming that no chemical descomposition take plase durring the films deposition process. Investigating the I-V characteristics of the realised structures on ITO it can be observed an improvement in the current value (\sim one order of magnitude) when a

supplementary layer of PEDOT:PSS was used in the standard structure. Also, an enhanced current can be achieved using an inverted structure, avoiding in this way the chemical interaction which can appear between the Al atoms and the organic layer.

Acknowledgments

This research was financially supported by the Romanian Ministry of Education and Research through National Core Founding Program, Contract No: 45N/27.02.2009, Bilateral Contract No. 783/25.06.2014, PCCA-2013-4-1439 and ID-PCE-2012-4-0467.

References

- [1] V. Kažukauskas, A. Arlauskas, M. Pranaitis, R. Lessmann, M. Riede, K. Leo, *Opt. Mat.* **32**(12), 1676 (2010).
- [2] A. Stanculescu, L. Vacareanu, M. Grigoras, M. Socol, G. Socol, F. Stanculescu, N. Preda, E. Matei, I. Ionita, M. Girtan, I.N. Mihailescu, *Appl. Surf. Sci.* **257**(12), 5298 (2011).
- [3] Wi Hyoung Lee and Yeong Don Park, *Polymers* **6**, 1057 (2014).
- [4] Seok Ju Kang, Gwan-Hyoung Lee, Young-Jun Yu, Yue Zhao, Bumjung Kim, Kenji Watanabe, Takashi Taniguchi, James Hone, Philip Kim and Colin Nuckolls, *Adv. Funct. Mater.* **24**(32), 5157 (2014).
- [5] Chizu Sekine, Yoshiaki Tsubata, Takeshi Yamada, Makoto Kitano and Shuji Doi, *Sci. Technol. Adv. Mater.* **15**, 034203 (2014).
- [6] Chih-Hao Chang, Ming-Kuan Hsu, Szu-Wei Wu, Mei-Hsin Chen, Hung-Hsuan Lin, Chia-Shou Li, Tun-Wen Pi, Hsin-Hua Chang and Nien-Po Chen, *Phys. Chem. Chem. Phys.* **17**, 13123 (2015).
- [7] A. Stanculescu, *J. Optoelectr. Adv. Materials* **9**(5), 1328 (2007).
- [8] A. Stanculescu, F. Stanculescu, *Thin Solid Films* **515**(24), 8733 (2007).
- [9] F. Stanculescu, A. Stanculescu, M. Socol, *J. Optoelectr. Adv. Materials* **8**(3), 1053 (2006).
- [10] F. Stanculescu, A. Stanculescu, M. Socol, *J. Optoelectr. Adv. Materials* **9**(5), 1352 (2007).
- [11] A. K. K. Kyaw, Y. Wang, D. W. Zhao, Z. H. Huang, X. T. Zeng and X. W. Sun, *Phys. Status Solidi A* **208**(11), 2635 (2011).
- [12] Chi-Feng Lin, Mi Zhang, Shun-Wei Liu, Tien-Lung Chiu and Jiun-Haw Lee, *Int. J. Mol. Sci.* **12**, 476 (2011).
- [13] Kazumi Yoshida, Takeo Oku, Atsushi Suzuki, Tsuyoshi Akiyama, Yasuhiro Yamasaki, *Adv. Chem. Engineer. Sci.* **2**, 461 (2012).
- [14] Debduitta Ray, Mauro Furno, Ellen Siebert-Henze, Karl Leo, and Moritz Riede, *Phys. Rev. B* **84**, 075214 (2011).
- [15] A. Stanculescu, F. Stanculescu, M. Socol, O. Grigorescu, *Solid State Sci.* **10**(12), 1762 (2008).
- [16] Darakhshan Qaiser, Mohd Shahid Khan, R.D. Singh, Zahid H. Khan, *Opt. Commun.* **283**, 3437 (2010).
- [17] S. Saito, A. Oshiyama, *Phys. Rev. Lett.* **66** (20), 2637 (1991).
- [18] Brian E. Lassiter, Guodan Wei, Siyi Wang, Jeremy D. Zimmerman, Viacheslav V. Diev, Mark E. Thompson, and Stephen R. Forrest, *Appl. Phys. Lett.* **98**, 243307 (2011).
- [19] Tomas Samuely, Shi-Xia Liu, Marco Haas, Silvio Decurtins, Thomas A. Jung and Meike Stöhr, *J. Phys. Chem. C* **113** (45), 19373 (2009).
- [20] Carolin R. Braatz, Gregor Öhl, and Peter Jakob, *J. Chem. Phys.* **136**(13), 134706 (2012).
- [21] Kouji Suemori, Yoshio Matsumura, Masaaki Yokoyama and Masahiro Hiramoto, *Jpn. J. Appl. Phys.* **45** (17), L472 (2006).
- [22] A. Stanculescu, G. Socol, M. Grigoras, T. Ivan, L. Vacareanu, M. Socol, O. Rasoga, C. Breazu, I. N. Mihailescu, I. Iordache, N. Preda, F. Stanculescu, *Appl. Phys. A* **117**(1), 261 (2014).

- [23] Kuwabara Takayuki, Nakayama Taketoshi, Uozumi Konosuke, Yamaguchi Takahiro, Takahashi Kohshin, *Sol. Energ. Mat. Sol. C* **92** (11), 1476 (2008).
- [24] Yu-Hong Lin, Po-Ching Yang, Jing-Shun Huang, Guo-Dong Huang, Ing-Jye Wang, Wen-Hao Wu, Ming-Yi Lin, Wei-Fang Su, Ching-Fuh Lin, *Sol. Energ. Mat. Sol. C* **95**(8), 2511 (2011).
- [25] A. Stanculescu, M. Socol, G. Socol, I. N. Mihailescu, M. Girtan, N. Preda, A.-M. Albu, F. Stanculescu, *Thin Solid Films* **520** (4), 1251 (2011).
- [26] G. Socol, A. C. Galca, C.R. Luculescu, A. Stanculescu, M. Socol, N. Stefan, E. Axente, L. Duta, C.M. Mihailescu, V. Craciun, D. Craciun, V. Sava, I.N. Mihailescu, *Dig. J. Nanomater. Bios.* **6** (1), 107 (2011).
- [27] R. Sathyamoorthy, S. Senthilarasu, *Sol Energy* **80**, 201 (2006).
- [28] Luciana Gaffo, Marcia R. Cordeiro, Adonilson R. Freitas, Wania C. Moreira, Emerson M. Giroto, Valtencir Zucolotto, *J. Mater. Sci.* **45**, 1366 (2010).
- [29] S Senthilarasu, S Velumani, R Sathyamoorthy, A Subbarayan, JA Ascencio, G Canizal, PJ Sebastian, JA Chavez, R Perez, *Appl. Phys. A* **77** (3-4), 383 (2003).
- [30] Haiyan Zhang, Chunyan Wu, Lizheng Liang, Yiming Chen, Yanyang He, Yanjuan Zhu, Ning Ke, J B Xu, S P Wong, Aixiang Wei and Shaoqi Peng, *J. Phys.: Condens. Matter* **13**, 2883 (2001).
- [31] Ivana Kopova, Lucie Bacakova, Vasily Lavrentiev and Jiri Vacik, *Int. J. Mol. Sci.* **14**, 9182 (2013).
- [32] B. M. Ginzburg, Sh. Tu İchiev, S. Kh. Tabarov, A. A. Shepelevski İ, L. A. Shibaev, *Techn. Phys.* **50** (11), 1458 (2005).
- [33] R Seoudi, GS El-Bahy, ZA El Sayed, *J. Mol. Struct.* **753** (1), 119 (2005).
- [34] Jibin Pu, Yufei Mo, Shanhong Wan and Liping Wang, *Chem. Commun.* **50**, 469 (2014).
- [35] Eduardo Rezende Triboni, Mauro Francisco Pinheiro da Silva, Alan Teruel Finco, Magali Aparecida Rodrigues, Grégoire Jean-François Demets, Fabio Henrique Dyszy, Paulo Celso Isolani, Pedro Berci Filho, Mario José Politi, *Mat.Res.* **13** (4), 505 (2010).
- [36] L. Torsi, A. Dodabalapur, N. Cioffi, L. Sabbatini, P.G. Zamboni, *Sens. Actuators B* **77** (1-2), 7 (2001).
- [37] S Senthilarasu, YB Hahn, SH Lee, *J. Appl. Phys.* **102** (4), 043512 (2007).
- [38] Ahalapitiya H. Jayatissa, Arunan Nadarajah and Achyut K. Dutta, *Proc. of SPIE* **6002**, 60021A-1 (2005).
- [39] Chih-Wei Chu, Yan Shao, Vishal Shrotriya, and Yang Yanga, *Appl. Phys. Lett.* **86**, 243506 (2005).
- [40] Christiane Falkenberg, Christian Uhrich, Selina Olthof, Bert Maennig, Moritz K. Riede, Karl Leo, *J. Appl. Phys.* **104**, 034506 (2008).
- [41] Hiroto, Tachikawa, Hiroshi Kawabata, Ryoji Miyamoto, Ken-ichi Nakayama, and Masaaki Yokoyama, *J. Phys. Chem. B* **109** (8), 3139 (2005).
- [42] M. Vogel, S. Doka, Ch. Breyer, M. Ch. Lux-Steiner, and K. Fostiropoulos, *Appl. Phys. Lett.* **89**, 163501 (2006).